MONOLITHIC S.A.W. CONVOLVERS USING CHIRP TRANSDUCERS

D P Morgan, D H Warne, P N Naish and D R Selviah

Plessey Research (Caswell) Ltd
Allen Clark Research Centre
Caswell Towcester Northants England

For optimum efficiency, the SAW elastic convolver requires efficient generation of narrow SAW beams. Dispersive transducers can be used for this purpose, since they can have small apertures without the inconvenience of high impedances, thus avoiding the need for beam compression. In convolvers, the dispersion can be arranged to cancel. A 300 MHz transducer was designed, with 110 MHz bandwidth and 57 μm aperture. A time-bandwidth product of 10 was chosen to give a radiation resistance near 50 ohm, as confirmed experimentally. A non-linear chirp characteristic was used to obtain a flat amplitude response without apodisation. A 12 μsec convolver with these transducers gave 110 MHz bandwidth and a -68 dBm bilinearity factor, using a dual-channel arrangement to give a spurious suppression of typically 35-40 dB. Results for this and other devices will be presented. Modified chirp transducers can be used to compensate for amplitude and phase errors produced elsewhere in the convolver. A new design compensates for dispersion due to the waveguide, and experimental results will be presented.

1. Introduction

The SAW elastic convolver provides a compact and inexpensive method for programmable correlation of coded waveforms for applications such as spread spectrum communications[1]. The device relies for its operation on a non-linear interaction in the substrate material, Y-Z lithium niobate. This interaction is rather weak, though it is well-established that improved efficiency is generally obtainable if the apertures of the SAW beams are minimised[2]. Recent devices have for this reason used apertures of a few wavelengths[3-6], the choice of aperture being influenced by waveguiding phenomena. For such devices, efficient generation of the narrow-aperture SAW beams is mandatory. This has been achieved through the use of multi-strip couplers[3,4] or beam-compressing metal horns [6]. In both cases, a relatively wide beam is generated by a conventional SAW transducer, and then compressed to an aperture of a few wavelengths before being launched in a SAW waveguide which constitutes the active non-linear part of the convolver.

In this paper we consider generation of narrow beams directly by using narrow-aperture transducers, so that beam compression is not used. Uniform SAW transducers with a few wavelengths aperture have high impedances and low capacitances, so that efficient transduction over a wide bandwidth is difficult and the performance is sensitive to stray capacitance. However, for a given acoustic bandwidth, a chirp transducer has a smaller impedance and a larger capacitance than a uniform transducer of the same aperture[7], and can therefore be used to overcome the disadvantages of a uniform transducer. We have found that convolvers using chirp transducers can give performance comparable with devices using beam compression. An advantage is that chirp transducers can be designed to compensate for amplitude or phase errors generated elsewhere in the convolver[8]. In addition, the narrow apertures enable the two waveguides of a dual-channel device to be located close together, so that their physical properties are closely similar.

2. Transducer Performance

We first show that the dispersion introduced by the chirp transducers can be arranged to cancel, so that is does not, in principle, affect the performance of the convolver. Consider the device of Fig. 1, consisting of two chirp transducers with a conventional parametric electrode between them. The applied waveforms are $v_S(t)$ and $v_R(t)$ with spectra $V_S(w)$ and $V_R(w)$ respectively. If the input transducers have frequency responses $H_S(w)$ and $H_R(w)$, the spectra of the waveforms entering the parametric electrode are $V_S(w) \cdot H_S(w)$ and $V_R(w) \cdot H_R(w)$. It is assumed that these waveforms have finite length and overlap only in the parametric region of the convolver, and also that the action of the parametric electrode is ideal. The output of the parametric electrode is therefore the convolution of the waveforms entering it, time-compressed by a factor of 2. In the frequency-domain, this is given by a product, with the frequency-scale expanded by a factor of 2. Thus the spectrum of the output waveform is

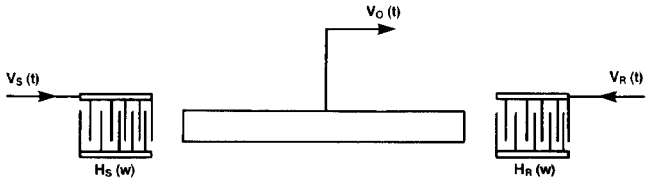

Figure 1

0090-5607/81/0000-0186 $00.75

$$V_o(w) = V_s(w/2) \cdot H_s(w/2) \cdot V_R(w/2) \cdot H_R(w/2) \qquad (1)$$

apart from a constant multiplier. The two transducers are taken to have the same geometry and to be oriented in the same direction. Ignoring circuit effects, the impulse responses will be the time-reverse of each other, and the frequency responses will be conjugates of each other. Thus $H_s(w) = H_R^*(w)$, and equn (1) becomes

$$V_o(w) = |H_R(w/2)|^2 \cdot V_R(w/2) \cdot V_s(w/2) \qquad (2)$$

This shows that the phase responses of the transducers have no effect on the output waveform, provided they are identical.

The required length of the transducer is determined by the impedance required. For the same acoustic bandwidth, a chirp transducer and a uniform transducer, with the same aperture, have impedances approximately in the ratio of the time-bandwidth product of the chirp transducer[7], with the chirp having the lower impedance. Assuming single-electrode transducers on Y-Z lithium niobate, a uniform transducer gives about 50 ohm radiation resistance if its aperture is 100 wavelengths. The radiation resistance of a chirp transducer is thus approximately 5000/(W.TB) ohm, where TB is the time-bandwidth product and W the aperture in wavelengths at the centre frequency. Here, the radiation resistance required was 100 ohm, since the dual-channel convolver uses pairs of transducers connected in parallel. The aperture was W = 5 wavelengths, somewhat larger than the 3 wavelength width of the waveguide because the guided mode has part of its energy propagating outside the metallised region. For these parameters the required TB-product is about 10. Thus, for a 100 MHz bandwidth the transducer dispersion is 100 nsec. For a 300 MHz centre frequency, the aperture is 57 μm and the capacitance is about 0.8 pF. For comparison, a uniform transducer with the same aperture and acoustic bandwidth would have a radiation resistance of 1000 ohm and a capacitance of 0.08 pF.

The chirp characteristics of the transducers were made somewhat non-linear in order to obtain a flat amplitude response without using apodisation. We define a time-domain phase $\theta(t)$ such that the electrode positions are given by t_n, where $\theta(t_n) = n\pi$, and the instantaneous frequency is

$$f_i(t) = \dot{\theta}(t)/2\pi \qquad (3)$$

Using the stationary-phase approximation, the conductance $G_a(f)$ of an unapodised chirp transducer is given by

$$G_a(f) \propto f^3 / |\ddot{\theta}(t_s)| \qquad (4)$$

where t_s is the stationary phase point, ie. the time at which the instantaneous frequency $f_i(t)$ of equn (3) is equal to f. Ignoring circuit effects, a flat amplitude response is obtained if $G_a(f)$ is constant within the pass-band, and the above equations then give

$$\theta(t) = A\sqrt{t - C_1} + C_2 \qquad (5)$$

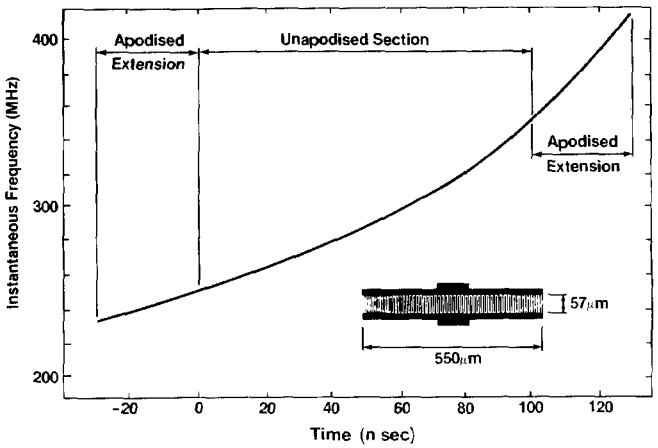

Figure 2

where A, C_1 and C_2 are constants. The value of A is determined by setting the instantaneous frequencies at the two ends of the transducer equal to the required band edge frequencies, making the difference of the corresponding times equal to the required transducer length. The constants C_1 and C_2 are inconsequential. Apodised extensions were added to each end in order to minimise ripples associated with the truncation. For the extensions, the electrode positions were obtained by extending the function $\theta(t)$ of equn (5) and sampling in the usual way. The above design method is based on the stationary-phase approximation and is thus strictly valid only for large TB-products. We have however, found the method to be effective for TB = 10, provided the extensions are long enough.

Figure 2 shows the instantaneous frequency (equn 3) for a transducer designed to give 100 MHz bandwidth centred at 300 MHz. The inset shows the physical appearance of the transducer. To compare the experimental and theoretical performance, transducers were made with this geometry scaled by a factor of 5, so that the centre frequency becomes 60 MHz and the bandwidth 20 MHz. Measurements of the series resistance are shown on Fig. 3, together with the theoretical series resistance and parallel conductance. The theoretical curves were obtained using charge superposition analysis[9] and do not allow for strays. The data refer to two identical transducers connected in parallel, as used in the convolver. The mid-band resistance is about 40 ohm, close to the intended 50 ohm, and the theoretical conductance is quite flat within the pass-band, as intended.

To test the transducer efficiency, a 300 MHz delay line was evaluated, using transducers connected in parallel at each end but without the electrode reversal used in dual-channel convolvers. Figure 4 shows the configuration . The transducers were modified slightly from the design of Figs.2 and 3 in order to increase the bandwidth to 120 MHz, though the aperture was 5 wavelengths (57 μm) as before. Waveguides were included, because tests of devices without waveguides showed appreciable extra losses due to diffraction. A 4-component matching circuit was used at each end. The measured insertion loss, Fig. 4, shows that the required 120 MHz bandwidth has been obtained, with

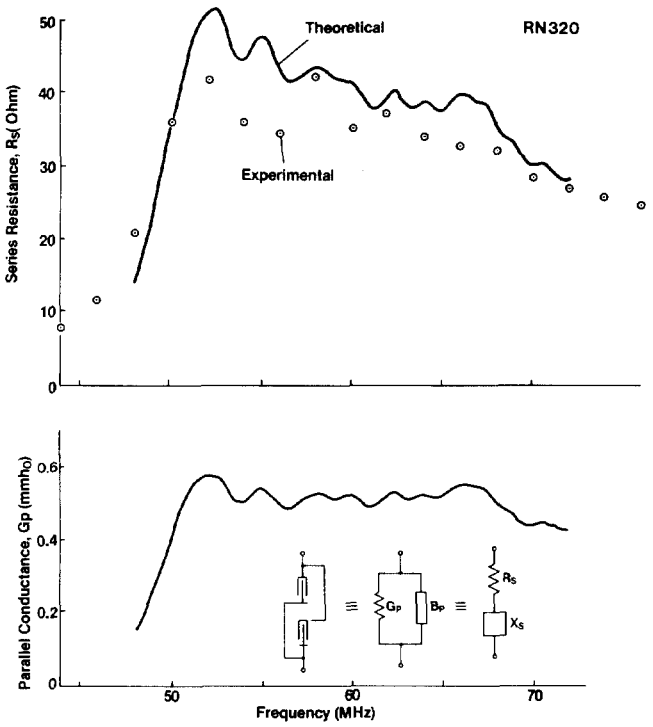

Figure 3

a mid-band insertion loss of 20 dB. The 3-dB roll-off is due to circuit effects not allowed for in the design, and is absent when no matching components are used.

An important issue is the power handling capability of the transducers, which is related to the maximum signal-to-noise ratio obtainable from a convolver. For a given acoustic power level, the voltage on the electrodes of a narrow-aperture chirp transducer will be similar to the voltage on the electrodes of a wide-aperture uniform transducer, because the impedances are similar. Thus if the breakdown is determined by the electrode voltage, the two transducer types should perform similarly. Experimental tests were performed on individual chirp transducers, applying 300 MHz CW waveforms. The transducers were

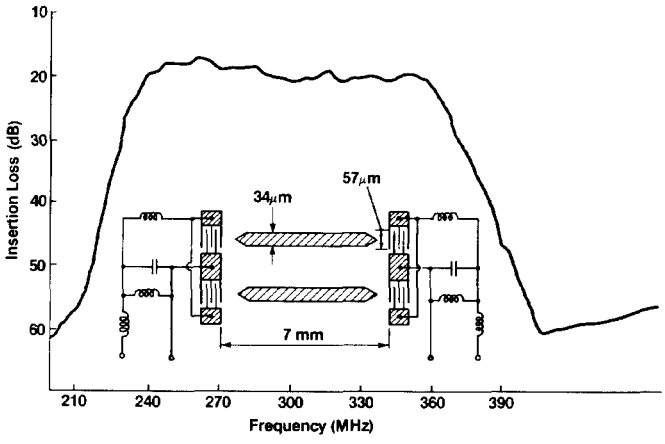

Figure 4

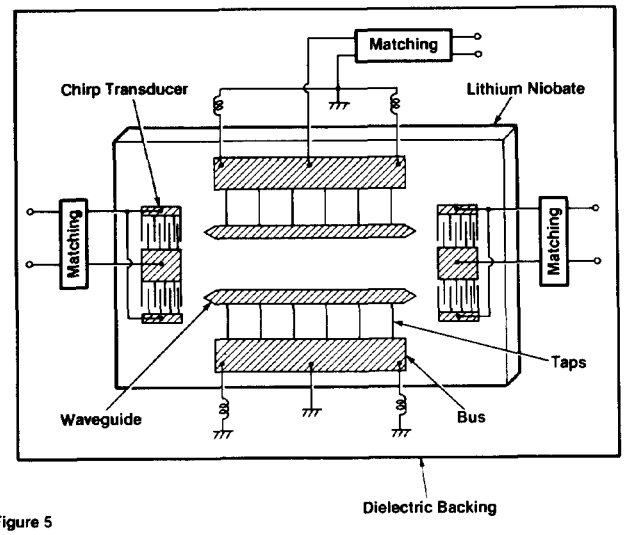

Figure 5

tuned using two inductors to give an impedance close to 50 ohm real. Breakdown occurred for input power levels of +32 dBm available from the 50 ohm source. This implies that for two identical transducers connected in parallel (as in the convolver) the breakdown level would be +35 dBm, which is similar to observations[4] for uniform transducers.

3. Convolver Design

The device configuration is shown schematically in Fig. 5. The contra-directed SAW beams are propagated in waveguides 34 μm wide (3 wavelengths at the centre frequency). This value is wide enough to minimise the dispersion of the fundamental mode, and narrow enough to restrict the number of possible propagating modes to two[10]. The first higher mode is antisymmetric and therefore is not excited in principle. The small amount of dispersion in the waveguides is beneficial in suppressing harmonic generation, which could otherwise cause saturation[5]. The end-to-end resistance of the waveguide is several hundred ohm. In order to provide a low-resistance path to the output port, each waveguide was connected to a wider bus-bar via a sequence of connecting strips referred to as taps, spaced about 4 mm apart.

In order to suppress reflections from the transducers, which would cause fold-over convolution, the dual-channel arrangement was used[11]. The convolver structure is duplicated, with the electrode polarities of one of the four input transducers reversed. Surface waves launched at one end of the structure generate voltages in anti-phase on the transducers at the other end, so that there is no net voltage produced, and hence reflections are suppressed as if the transducers were shorted. The reflection suppression is in principle independent of frequency. An additional advantage is that output signals generated by the input transducers are suppressed - such output signals could be reflected in the external circuitry so that they are re-applied to the convolver giving an additional spurious signal at the convolver output. The dual-channel arrangement does not however suppress reflections due to the mass and electrical loading of the electrodes.

In the dual-channel arrangement, a non-linear interaction takes place in each of the two waveguides, and for optimum efficiency both interactions should contribute to the output signal. If the waveguides were far apart, a voltage would be developed between each waveguide and a ground plane at the rear of the crystal, as in a conventional single channel convolver. These two voltages are in anti-phase, and can therefore be summed in a balun transformer[6]. The approach used here is somewhat different, avoiding the need for the transformer. If the rear face of the crystal is not grounded, then contra-directed waves in one of the waveguides give a non-linear output voltage developed between the two waveguides; the waveguide which is not supporting surface waves acts as a ground electrode on the surface, as in some single-channel convolver designs[3,4]. Surface waves in the other waveguide give a voltage with the opposite polarity, owing to the reversal of one of the transducers, but the voltage between the waveguides has the same polarity. Thus when SAW's are present in both waveguides, the voltage between them is the sum of contributions from the interactions in individual waveguides. To extract this voltage, one of the waveguides is grounded, and the other is connected to the output port (Fig. 5). The method is effective only if the capacitance between the waveguides is larger than the capacitance between the 'live' waveguide and the ground; in practice, the latter is mainly due to the capacitance of the live bus-bar. To satisfy this condition, it is usually necessary to mount the lithium niobate crystal over a dielectric layer, which has a much lower dielectric constant than lithium niobate (typically 4 instead of 46). In our devices, the efficiencies were found to be typically 12 dB worse if the dielectric layer was omitted. Close spacing of the waveguides increases the capacitance between them, thus reducing the effect of the stray capacitance of the bus-bar. On the other hand acoustic coupling (10) must be avoided, so that the choice of waveguide separation is a compromise between these two factors. For our devices, the separation was 170 to 200 μm, though this could probably be reduced.

4. Convolver Performance

Several convolver designs have been investigated, and we report mainly on a design with a 16 μsec interaction length and 120 MHz input bandwidth, centred at 300 MHz. The transducer design was as in the delay line experiment of Fig. 4. The ends of the bus-bars were grounded via small inductors (Fig. 5), in order to minimise variations in the interaction uniformity due to transmission line effects[12]. The input transducers were matched using 4-component circuits, as in Fig. 4, which improved the convolver efficiency by about 6 dB as compared with series inductor tuning. A two-component circuit was used at the output port to improve the VSWR, though this did not affect the device efficiency much. The device was mounted in a brass package 120 x 20 x 8 mm (excluding connectors) and is shown in Fig. 6.

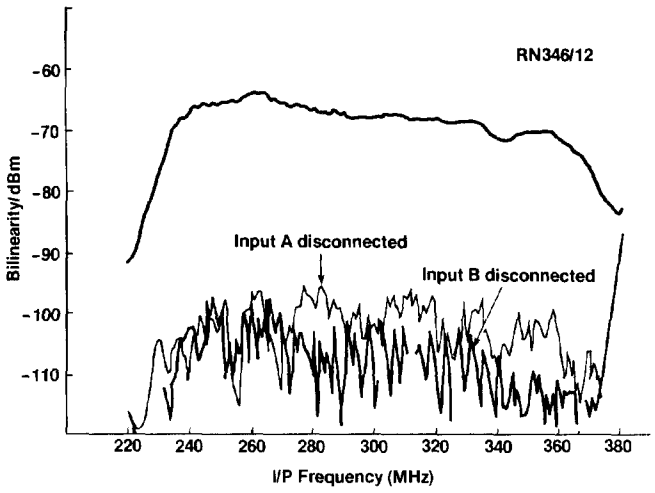

Figure 7

The bilinearity factor of one of these devices, as a function of frequency, is shown in the upper curve of Fig. 7. This curve was obtained by inserting CW waveforms at the same frequency to the two input ports, and measuring the output amplitude using a vector voltmeter. The reference for the vector voltmeter was obtained by applying the input waveform to a frequency doubler. Prior to the convolver measurement, the gains of the input and output circuits were calibrated as functions of frequency. The bilinearity factor is defined as 10 log $(P_o/P_1 . P_2)$ dBm, where P_1 and P_2 are the input powers available from 50 ohm sources and P_o is the output power delivered to a 50 ohm load, with all three powers referring to rms values measured in mW. At the centre frequency, the measured bilinearity factor was -67 dBm.

The lower two curves on Fig. 7 were obtained by repeating the measurement with one of the two convolver inputs disconnected. These curves give the spurious levels of the device, due mainly to fold-over convolution. The peak level of the spurious is typically 30 to 35 dB below the main output signal, depending somewhat on the frequency and on which input port is used.

These results are typical of a number of devices, when matched with appropriate circuits. For most

Figure 6

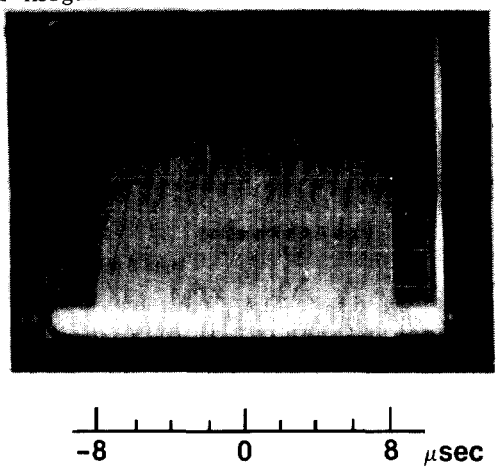

Figure 8

devices, the bilinearity curves were found to have very similar shapes, with the centre-frequency value varying over a range of -65 to -69 dBm. The spurious suppression was somewhat less repeatable. Similar repeatability was obtained for devices with 12 μsec interaction length, designed for 100 MHz input bandwidth. These devices gave similar efficiencies and spurious suppression.

Figure 8 shows the interaction uniformity for the same 16 μsec device as Fig. 7. This was obtained by applying 0.1 μsec RF pulses with centre frequency 300 MHz to the two convolver inputs. The input pulses were generated using two pulse generators without synchronisation, so that the relative times are randomised and the pulses overlap at random positions within the interaction region; with a sufficient exposure time, the amplitude is obtained for all locations in the parametric region. This method gives better sensitivity than the more usual technique in which a long pulse is applied at one end, because spurious signals are reduced. Experimentally, the amplitude varies by about ± 0.9 dB, and shows dips corresponding to the locations of the tapping points. This result is typical of the 16 μsec devices, and did not vary much with the centre frequency of the input pulses.

Figure 9 shows convolver output waveforms for correlation of a linear FM chirp signal. Here the convolver input waveforms were generated by impulsing a SAW expander and compressor which were designed to be used as a pair in a radar system, with 11 MHz bandwidth and 14 μsec pulse duration. The compressor was weighted to suppress time-sidelobes. The waveforms were up-converted from 70 MHz centre frequency into the convolver band. The top trace of Fig. 9 shows the compressed pulse produced by the convolver, and the centre trace is the same waveform with an expanded timescale. For the third trace, the level of one of the input signals was reduced by 50 dB and additional amplification was applied at the output. The compressed pulse is still clearly visible above the noise and spurious signals, showing that a large dynamic range is achievable.

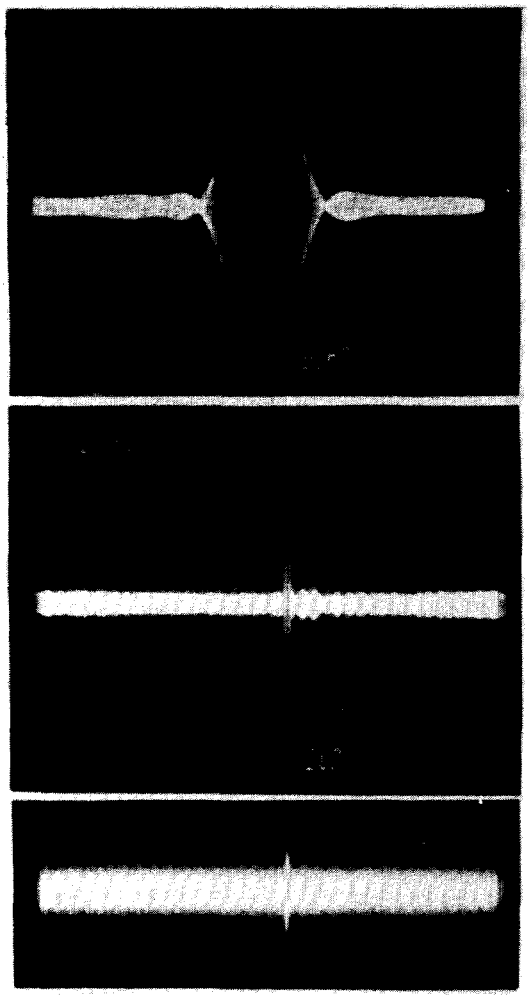

Figure 9

5. Modified Transducers for Phase-Error Compensation

In the frequency domain, the convolver output contains a phase error term corresponding to the dispersion produced by the waveguides, and this is the largest source of phase errors in this type of convolver[13]. The error can however be reduced by modifying the chirp transducers so that they have slightly different dispersions[8]. Consider an individual chirp transducer, with time-domain phase $\theta(t)$ as in section 2 above. The phase response in the frequency domain is $\phi(w)$, and the transducer is to be re-designed so that the new phase response is $\phi(w) + \Delta\phi(w)$, where $\Delta\phi(w)$ is the required phase change. The new design requires a new time-domain phase $\theta_1(t)$. If $\Delta\phi(w)$ is small enough, $\theta_1(t)$ is given by[8]

$$\theta_1(t) = \theta(t) + \Delta\phi\left[\dot{\theta}(t)\right] \qquad (6)$$

Thus any required phase change can be produced in principle. Although equn (6) is based on the stationary-phase approximation, we have found this technique to be effective for time-bandwidth products of only 10, as required for our convolvers.

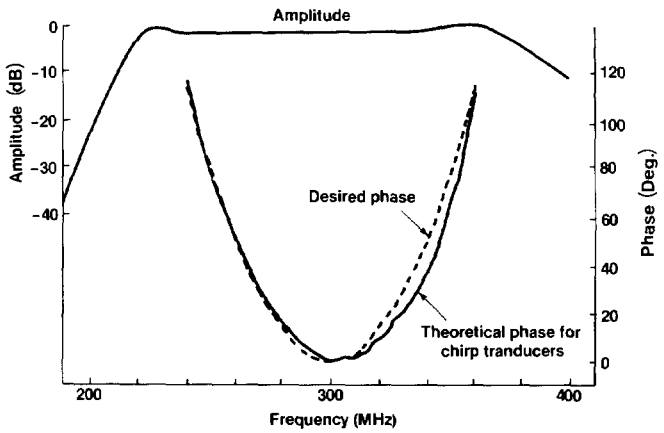

Figure 10

The phase error produced by the waveguides is roughly quadratic with frequency. A modified design was produced, with the transducers designed to give a quadratic phase error varying by 115° over the 120 MHz band. Each transducer was designed to give half of this error, so that one transducer was somewhat longer than the original design and the other was shorter. Figure 10 shows results of a delta-function analysis of the response, for the two transducers combined, showing that the theoretical phase agrees quite closely with the desired (quadratic) curve.

The phase responses of two convolvers are shown in Fig. 11, where one curve is for a conventional 16 μsec device as discussed in section 4 above, and the other curve is for a device using the phase-compensating transducers. These curves were obtained by inserting CW waveforms into both convolver inputs and measuring the phase of the convolver output on a vector voltmeter, with the reference for the vector voltmeter obtained by using a frequency doubler.

6. Conclusions

Experimental work has shown that chirp transducers with 5 wavelengths aperture and a TB-product of 10 give impedances similar to uniform transducers with the same bandwidth and with apertures 10 times larger, and that delay lines with such transducers can give 20 dB insertion loss and 120 MHz bandwidth. Convolvers using such transducers have performance similar to devices using horn or multi-strip beam compressors, and a -67 dBm bilinearity factor was obtained for a 16 μsec device. The use of chirp transducers avoids the need for beam compression, so that the devices are more compact and the fabrication difficulty associated with the long narrow strips of a multi-strip compressor is avoided. In addition, chirp transducers can be designed to compensate for amplitude or phase errors arising elsewhere in the convolver, and compensation for phase errors due to the dispersion of the waveguides was demonstrated experimentally.

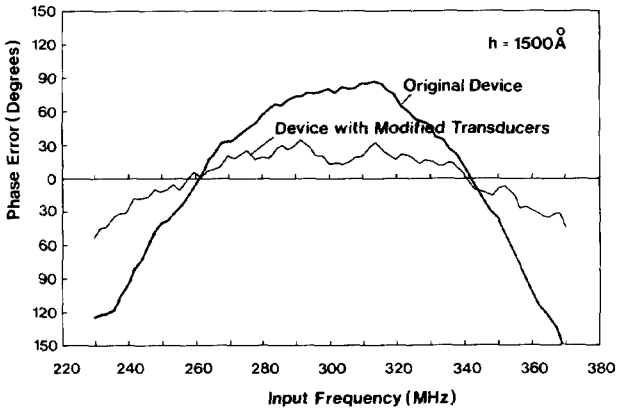

Figure 11

Acknowledgements

It is a pleasure to acknowledge technical contributions from B Lewis and R K Chapman and, for device fabrication, from R M Gibbs. We also thank M F Lewis and G F Moule for helpful discussions and for obtaining the phase measurements of Fig. 11. This work has been carried out with the support of the Procurement Executive, Ministry of Defence, sponsored by DCVD.

References

1) D P Morgan, Ultrasonics, 12, 74-83 (1974).

2) M Luukkala and J Surakka, J Appl Phys, 43, 2510-2518 (1972).

3) P Defranould and C Maerfeld, Proc IEEE, 64, 748-751 (1976).

4) H Gautier and C Maerfeld, IEEE Ultrasonics Symp, 1980, p.30-36.

5) B J Darby, D Gunton and M F Lewis, ibid, p.53-58.

6) I Yao, ibid, p.37-42.

7) C S Hartmann, D T Bell and R C Rosenfeld, IEEE Trans, MTT-21, 162-175 (1973).

8) W R Smith, IEEE Ultrasonics Symp, 1980, p.59-64.

9) B Lewis, P M Jordan, R F Milsom and D P Morgan, IEEE Ultrasonics Symp, 1978, p.709-714.

10) R V Schmidt and L A Coldren, IEEE Trans, SU-22, 115-122 (1975).

11) Work previously unreported, conducted at University of Edinburgh, 1973, supported by the Ministry of Defence and sponsored by DCVD.

12) J H Goll and R C Bennett, IEEE Ultrasonics Symp, 1978, p.44-47.

13) D P Morgan, IEEE Trans, SU-22, 274-277 (1975) and E L Adler and J H Cafarella, IEEE Ultrasonics Symp, 1980, p.1-4.